

# Heavy Supersymmetric Particle Effects in Higgs Boson Production Associated with a Bottom Quark Pair at LHC and Tevatron

Guangping Gao

*Institute of Theoretical Physics, Academia Sinica, Beijing 100080, China*

Robert J. Oakes

*Department of Physics and Astronomy, Northwestern University, Evanston, IL 60208, USA*

Jin Min Yang

*CCAST(World Laboratory), P.O.Box 8730, Beijing 100080, China;*

*Institute of Theoretical Physics, Academia Sinica, Beijing 100080, China*

If all the supersymmetry particles (sparticles) except a light Higgs boson are too heavy to be directly produced at the Large Hadron Collider (LHC) and Tevatron, a possible way to reveal evidence for supersymmetry is through their virtual effects in other processes. We examine such supersymmetric QCD effects in bottom pair production associated with a light Higgs boson at the LHC and Tevatron. We find that if the relevant sparticles (gluinos and squarks) are well above the TeV scale, too heavy to be directly produced, they can still have sizable virtual effects in this process. For large  $\tan\beta$ , such residual effects can alter the production rate by as much as 40 percent, which should be observable in future measurements of this process.

14.80.Ly, 14.80.Cp, 12.60.Jv

## I. INTRODUCTION

Searching for the Higgs boson is one of the most important tasks in particle physics. The existence of a relatively light Higgs is suggested by high precision fits to the data in the Standard Model (SM) and also is theoretically favored in the Minimal Supersymmetric Standard Model (MSSM) [1]. Verification of the existence of a light Higgs boson at the LHC or Tevatron is therefore a very important test for both the SM and the MSSM. Among the various production channels for a light Higgs boson at the hadron colliders, the production in association with a bottom quark pair,  $pp(\text{or } p\bar{p}) \rightarrow hbb + X$ , plays an important role in testing the bottom quark Yukawa couplings. While this process has a small cross section in the SM, in the MSSM this production mechanism can be a significant source of Higgs bosons since the bottom quark Yukawa coupling in the MSSM is proportional to  $\tan\beta$  (defined as  $v_2/v_1$  with  $v_{1,2}$  being the vacuum expectation values of the two Higgs doublets) and the current analyses favor large  $\tan\beta$ . This process has been studied at next-to-leading order in perturbative QCD [2–8]. Due to the importance of this production mechanism in testing the bottom quark Yukawa coupling in the MSSM, the supersymmetry (SUSY) loop effects in this process should also be considered. Of course, among the SUSY loop effects the one-loop SUSY QCD corrections are the dominant.

In the present work we examine the one-loop SUSY QCD effects in this process. Instead of performing a complete one-loop calculation, which would be quite complicated since it involves many five-point box diagrams, we focus on the so-called SUSY residual effects, i.e., the SUSY effects in the heavy limit ( $\gtrsim$  TeV) of the sparticles involved. Our motivations are the following:

- It is possible that all the sparticles except a light Higgs boson are too heavy to be directly produced at the LHC and Tevatron, such as in the split SUSY scenario proposed recently by Arkani-Hamed and Dimopoulos [9]. Although the fermionic partners (gauginos and Higgsinos) in this scenario are required to be relatively light in

order to ensure gauge coupling unification and provide dark matter candidates, they are not necessarily below a TeV, as recently shown [10]. Thus, it is possible for the LHC and Tevatron to observe no sparticles except a light Higgs boson. In that case a possible way to reveal a hint of supersymmetry is through its residual effects in observable processes.

- Unfortunately (or fortunately), SUSY virtual effects decouple in most processes when SUSY particles become very heavy. However, we know that the only processes where SUSY has residual effects are those processes involving Higgs-fermion Yukawa couplings, as first studied for  $h \rightarrow b\bar{b}$  decay [11,12], and also for certain production processes [13,14]. The production reaction  $pp(\text{or } p\bar{p}) \rightarrow h b\bar{b} + X$  at the LHC or Tevatron is well suited for revealing SUSY residual effects since it involves the  $h b\bar{b}$  coupling. Compared with  $pp(\text{or } p\bar{p}) \rightarrow h b + X$ , this process is also easier to detect since it contains an extra hard  $b$  jet in the final state. Once the Higgs boson ( $h$ ) is observed and its mass is measured through other processes such as gluon-gluon fusion, this reaction can be used to measure the bottom quark Yukawa coupling and to observe the expected residual effects of SUSY.

Note that the existence of SUSY residual effects in some Higgs process does not mean SUSY is not decoupling in low energy processes. As shown in previous studies, and also in the following work, the residual effects exist when  $M_A$  remains light; when  $M_A$  is heavy, together with all other SUSY masses, the residual effects do vanish.

This paper is organized as follows: In Section II we present our strategy for the calculation of the one-loop SUSY QCD corrections. In Section III we perform numerical calculations and obtain the residual effects in the limit of heavy SUSY masses. The conclusion is given in Section IV and the detailed analytic formulas obtained in our calculations are presented in the Appendix.

## II. ONE-LOOP SUSY QCD CORRECTIONS

The production  $pp(\text{or } p\bar{p}) \rightarrow h b\bar{b} + X$  proceeds through the parton-level processes  $gg \rightarrow h b\bar{b}$  and  $q\bar{q} \rightarrow h b\bar{b}$ . The one-loop SUSY QCD corrections to this process have a huge number of one-loop diagrams, including many five-point box diagrams. However, among all these diagrams only the one-loop diagrams involving the bottom quark Yukawa coupling have residual effects as the SUSY masses become very heavy. Therefore, in our calculation we need only consider the loop corrected bottom quark Yukawa coupling diagrams shown in Fig. 1 and Fig. 2.

In our loop calculations we used dimensional regularization to control the ultraviolet divergences and adopted the on-mass-shell renormalization scheme. Each effective  $h b\bar{b}$  vertex in Fig.1 contains two parts: one is the irreducible three-point vertex loop contributions and the other is the counterterms  $\delta V_{hb\bar{b}} = g_{hb\bar{b}}^0 \delta Z$  with  $g_{hb\bar{b}}^0$  denoting the tree-level  $h b\bar{b}$  coupling and  $\delta Z$  is the renormalization constant given by

$$\delta Z = \frac{\delta Z_L}{2} + \frac{\delta Z_R}{2} + \frac{\delta m_b}{m_b}, \quad (1)$$

where  $\delta Z_{L,R}$  and  $\delta m_b$  are respectively the renormalization constant for the  $b$  quark field and mass. They can be extracted from the one-loop self-energies shown in Fig. 2(b) by using the on-mass-shell renormalization condition. They are given by

$$\delta Z_L = \sum_{i=1}^2 \left[ \left( 2m_b^2 A_i^1 \frac{\partial B_1}{\partial p_b^2} - 2m_b m_{\tilde{g}} A_i^2 \frac{\partial B_0}{\partial p_b^2} \right) \Big|_{p_b^2=m_b^2} + (A_i^1 - A_i^3) B_1 \right] (m_b^2, m_{\tilde{g}}^2, m_{b_i}^2), \quad (2)$$

$$\delta Z_R = \delta Z_L \Big|_{A_i^3 \rightarrow -A_i^3}, \quad (3)$$

$$\frac{\delta m_b}{m_b} = \left( \frac{m_{\tilde{g}}}{m_b} A_i^2 B_0 - A_i^1 B_1 \right) (m_b^2, m_{\tilde{g}}^2, m_{b_i}^2), \quad (4)$$

where  $A_i^1 = a_i^2 + b_i^2$ ,  $A_i^2 = a_i^2 - b_i^2$  and  $A_i^3 = 2a_i b_i$  with  $a_i$  and  $b_i$  given in the Appendix.  $B_{0,1}$  are the 2-point Feynman integrals given in [15], and their functional dependence is indicated in the brackets following them.

The counterterm is universal for each  $h b\bar{b}$  vertex shown in Fig. 1. However, although the irreducible three-point vertex loops have the same topological structure shown in Fig. 2(a), the results are different for different  $h b\bar{b}$  vertices in Fig. 1 because they depend on the external momenta. The results are lengthy and are presented in the Appendix. We have checked that all the ultraviolet divergences do cancel as a result of renormalizability of the MSSM.

Note that in our calculations we adopted the so-called on-mass-shell scheme, in which the renormalized mass  $m_b = m_b^0 - \delta m_b$  ( $m_b^0$  is the bare mass) is the physical mass, i.e., the pole of the  $b$ -quark propagator [11,16,17]. The

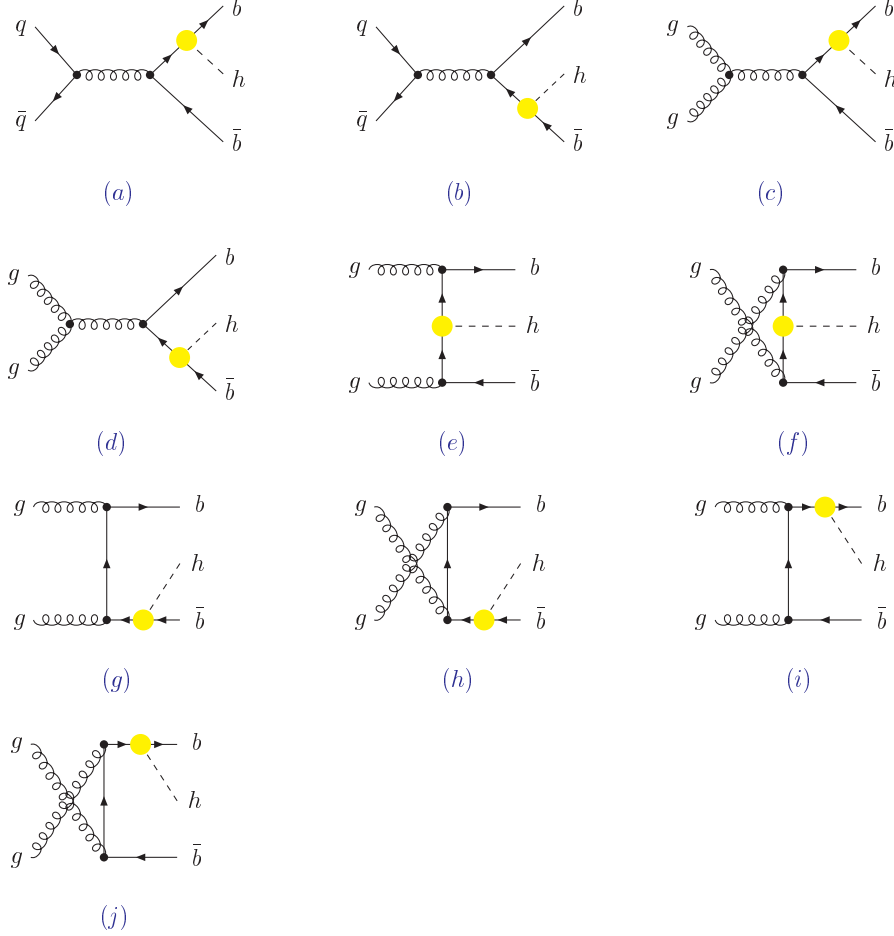


FIG. 1. Feynman diagrams for parton-level subprocesses for  $pp(\text{or } p\bar{p}) \rightarrow h b \bar{b} + X$  with one-loop SUSY QCD corrected  $h b \bar{b}$  vertices. The large dots denote the effective  $h b \bar{b}$  vertex with one-loop SUSY QCD corrections.

main difference of this scheme with the  $\overline{MS}$  scheme is that in the  $\overline{MS}$  scheme a running b-quark mass is introduced to absorb the leading part of the corrections (for example, the large logarithms in QCD corrections) [16]. In calculating SUSY-QCD corrections, there are no such large logarithms and the on-mass-shell scheme is usually adopted (an extensive discussion about this issue was provided in [17])<sup>1</sup>.

Including the one-loop SUSY-QCD corrections to the bottom quark Yukawa coupling, the renormalized amplitude for  $pp(\text{or } p\bar{p}) \rightarrow h b \bar{b} + X$  can be written as

$$M = M_0^{q\bar{q}} + \delta M^{q\bar{q}} + M_0^{gg} + \delta M^{gg}, \quad (5)$$

where  $M_0$  and  $\delta M$  represent the tree-level amplitude and one-loop SUSY-QCD corrections, respectively. The detailed expression for  $\delta M$  is given in the Appendix.

In our calculation we performed Monte Carlo integration to obtain the hadronic cross section by using the CTEQ5L

<sup>1</sup>If we use the  $\overline{MS}$  scheme in calculating SUSY-QCD corrections to the  $h b \bar{b}$  coupling, i.e., define a running b-quark mass to absorb some SUSY-QCD correction effects, we will obtain the approximately same result for the ratio of the cross sections with and without SUSY-QCD corrections (because by doing this we merely relocated some correction effects and the total one-loop SUSY-QCD correction effects are not changed).

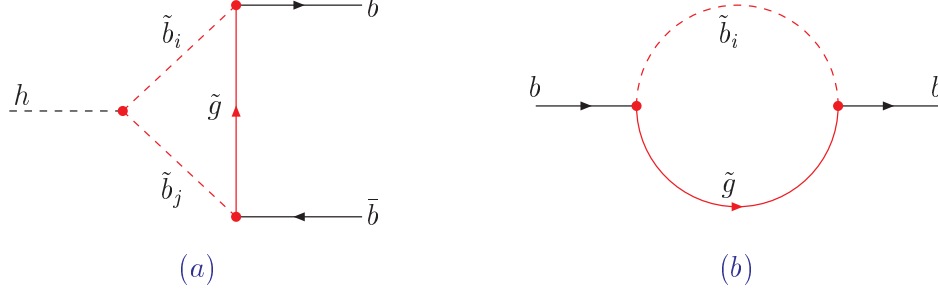


FIG. 2. Feynman diagrams for the one-loop SUSY QCD corrections to the  $h b \bar{b}$  vertex: (a) the irreducible vertex loops and (b) the self-energy loops of the  $b$  quark.

parton distribution functions [18] with  $Q = m_h$  and requiring the transverse momentum of the two  $b$ -jets to be larger than 15 GeV.

To exhibit the size of the corrections we define the ratio

$$\Delta_{SQCD} = \frac{\sigma - \sigma_0}{\sigma_0} , \quad (6)$$

where  $\sigma_0$  is the tree-level cross section.

### III. NUMERICAL RESULTS

Before performing numerical calculations, we must choose the parameters involved. For the SM parameters we used  $m_W = 80.448$  GeV,  $m_Z = 91.187$  GeV,  $m_t = 178$  GeV,  $m_b = 4.5$  GeV,  $\sin^2 \theta_W = 0.223$ , and the two-loop running coupling constant  $\alpha_s(Q)$ . For the SUSY parameters, apart from the charged Higgs mass, gluino mass and  $\tan \beta$ , the mass parameters of sbottoms are involved. The mass-squared matrix for the sbottoms takes the form [19]

$$M_b^2 = \begin{pmatrix} m_{b_L}^2 & m_b X_b^\dagger \\ m_b X_b & m_{b_R}^2 \end{pmatrix} , \quad (7)$$

where

$$m_{b_L}^2 = m_{\tilde{Q}}^2 + m_b^2 - m_Z^2 \left( \frac{1}{2} - \frac{1}{3} \sin^2 \theta_W \right) \cos(2\beta) , \quad (8)$$

$$m_{b_R}^2 = m_{\tilde{D}}^2 + m_b^2 - \frac{1}{3} m_Z^2 \sin^2 \theta_W \cos(2\beta) , \quad (9)$$

$$X_b = A_b - \mu \tan \beta , \quad (10)$$

Here  $m_{\tilde{Q}}^2$  and  $m_{\tilde{D}}^2$  are soft-breaking mass terms for the left-handed squark doublet  $\tilde{Q}$  and the right-handed down squark  $\tilde{D}$ , respectively.  $A_b$  is the coefficient of the trilinear term  $H_1 \tilde{Q} \tilde{D}$  in the soft-breaking terms and  $\mu$  is the bilinear coupling of the two Higgs doublets in the superpotential. Thus, the SUSY parameters involved in the sbottom mass matrix are  $m_{\tilde{Q}}$ ,  $m_{\tilde{D}}$ ,  $A_b$ ,  $\mu$  and  $\tan \beta$ .

The mass-squared matrix is diagonalized by a unitary transformation which relates the weak eigenstates  $\tilde{b}_{L,R}$  to the mass eigenstates  $\tilde{b}_{1,2}$ :

$$\begin{pmatrix} \tilde{b}_1 \\ \tilde{b}_2 \end{pmatrix} = \begin{pmatrix} \cos \theta_b & \sin \theta_b \\ -\sin \theta_b & \cos \theta_b \end{pmatrix} \begin{pmatrix} \tilde{b}_L \\ \tilde{b}_R \end{pmatrix} \quad (11)$$

with the mixing angle and masses determined by

$$m_{\tilde{b}_{1,2}} = \frac{1}{2} \left[ m_{\tilde{b}_L}^2 + m_{\tilde{b}_R}^2 \mp \sqrt{(m_{\tilde{b}_L}^2 - m_{\tilde{b}_R}^2)^2 + 4m_b^2 X_b^2} \right], \quad (12)$$

$$\tan 2\theta_b = \frac{2m_b X_b}{m_{\tilde{b}_L}^2 - m_{\tilde{b}_R}^2}. \quad (13)$$

In addition, we consider the following experimental constraints:

- (1)  $\mu > 0$  and large  $\tan \beta$ , in the range  $5 \leq \tan \beta \leq 50$ , which are favored by the recent muon  $g-2$  measurement [20].
- (2) The LEP and CDF lower mass bounds on gluino and sbottom [21]

$$m_{\tilde{b}_1} \geq 75.0 \text{ GeV}, \quad m_{\tilde{g}} \geq 190 \text{ GeV}. \quad (14)$$

Next, we present numerical results for LHC ( $\sqrt{s} = 14 \text{ TeV}$ ) and Tevatron ( $\sqrt{s} = 2 \text{ TeV}$ ) in two representative cases:

*Case A:* All SUSY mass parameters are of the same size and much heavier than the weak scale, but  $M_A$  is fixed at weak scale, i.e.,

$$M_{SUSY} \equiv M_{\tilde{Q}} = M_{\tilde{D}} = A_b = M_{\tilde{g}} = \mu \gg M_{EW}. \quad (15)$$

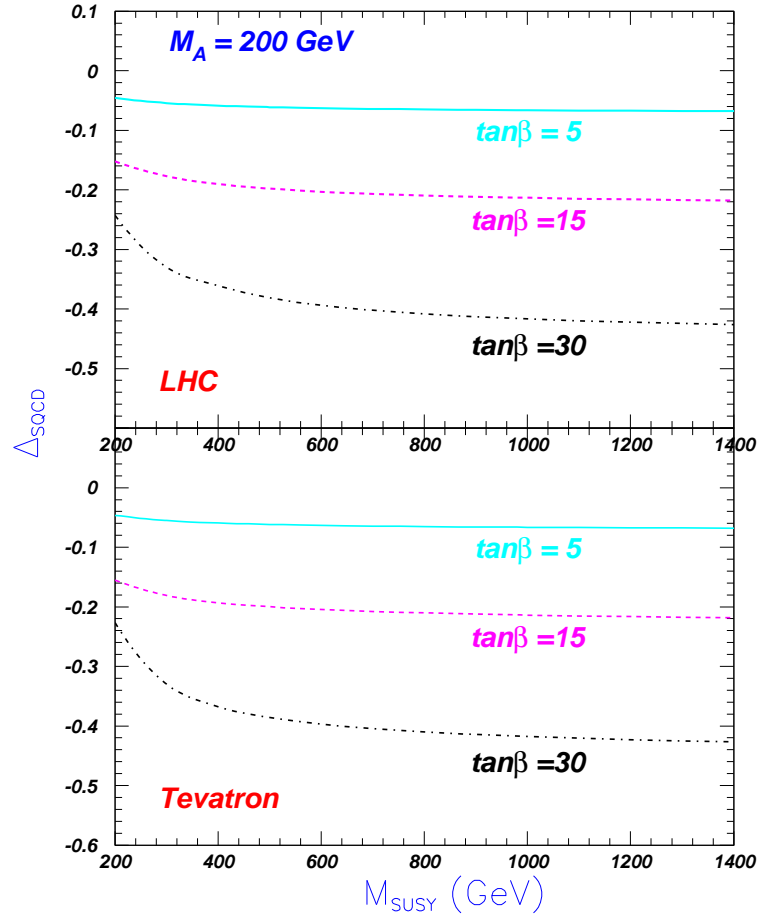


FIG. 3. SUSY QCD effects  $\Delta_{SQCD} = (\sigma - \sigma_0)/\sigma_0$  versus the common SUSY mass  $M_{SUSY} (\equiv M_{\tilde{Q}} = M_{\tilde{D}} = A_b = M_{\tilde{g}} = \mu)$  for a fixed  $M_A$  and different values of  $\tan \beta$ . The corresponding range of  $m_h$  is  $94 \sim 113 \text{ GeV}$  for  $\tan \beta = 5$ ,  $102 \sim 121 \text{ GeV}$  for  $\tan \beta = 15$  and  $103 \sim 122 \text{ GeV}$  for  $\tan \beta = 30$ .

In this case the mixing of sbottoms is maximal, i.e.,  $\theta_b \sim \pm \pi/4$ . Figs. 3 and 4 show the dependence on the SUSY scale  $M_{SUSY}$  for different values of  $\tan \beta$  and  $M_A$ . We see that  $\Delta_{SQCD}$  approaches a non-vanishing constant as

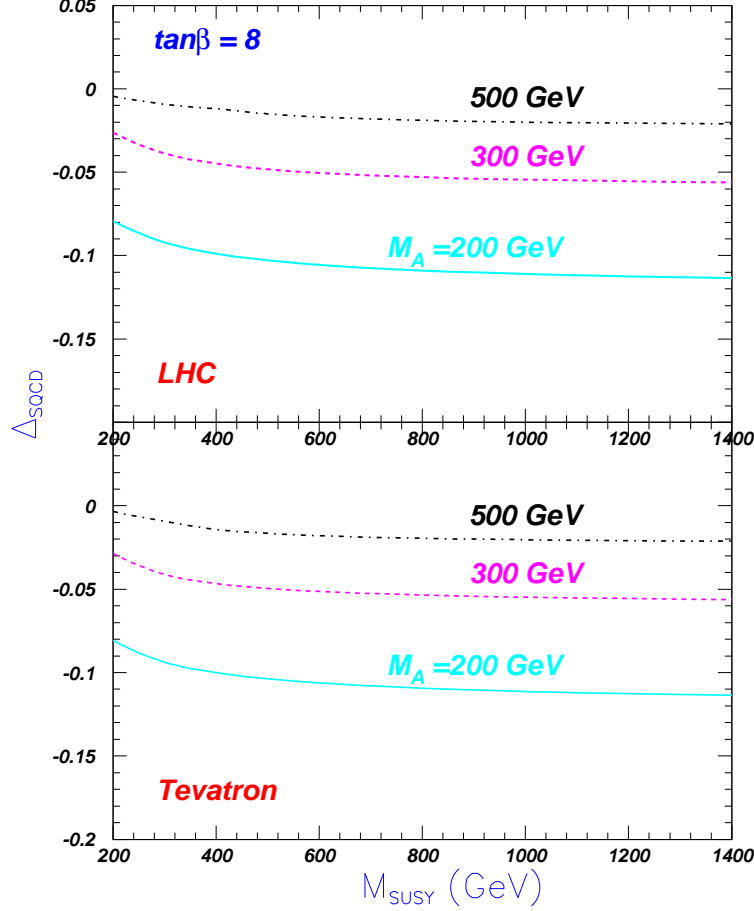


FIG. 4. Same as Fig.3 but for a fixed value of  $\tan\beta$  and different values of  $M_A$ . The corresponding range of  $m_h$  is  $99 \sim 118$  GeV for  $m_A = 200$  GeV,  $100 \sim 119$  GeV for  $m_A = 300$  GeV and  $100 \sim 120$  GeV for  $m_A = 500$  GeV.

$M_{SUSY}$  becomes large. The effects are enhanced by  $\tan\beta$ . For  $\tan\beta = 30$ , the residual effects can be as large as 40%<sup>2</sup>. Fig. 4 shows that as  $M_A$  becomes large the size of residual effects decrease.

*Case B:* All SUSY mass parameters, including  $M_A$ , are much larger than the weak scale, i.e.,

$$M_{SUSY} \equiv M_{\tilde{Q}} = M_{\tilde{D}} = A_b = M_{\tilde{g}} = \mu = M_A \gg M_{EW} . \quad (16)$$

This case also gives maximal mixing for sbottoms. In Fig. 5 we show the dependence on the MSSM mass scale  $M_{SUSY}$ . This figure explicitly exhibits the decoupling behaviour of SUSY QCD as  $M_{SUSY}$  becomes large.

The underlying reason for the existence of SUSY residual effects in fermion Yukawa couplings when  $M_A$  is fixed at the weak scale is that certain couplings are proportional to SUSY mass parameters [22]. As pointed out in [23], the SUSY QCD residual effects in the  $h\bar{b}b$  coupling are proportional to  $\tan\beta$ . For  $ht\bar{t}$  coupling, however, the SUSY QCD residual effects are proportional to  $\cot\beta$ . For the process  $pp(\text{or } p\bar{p}) \rightarrow ht\bar{t} + X$  the calculation of SUSY QCD corrections is analogous to the  $pp(\text{or } p\bar{p}) \rightarrow h\bar{b}b + X$  case. However, we found that the SUSY residual effects in  $pp(\text{or } p\bar{p}) \rightarrow ht\bar{t} + X$  are quite small, reaching only 3% for  $\tan\beta = 5$  and being smaller for larger  $\tan\beta$  values. Such a small effect is even less than the next-to-leading-order QCD corrections [24–29] and is not likely to be observed at the LHC or Tevatron.

<sup>2</sup>Note that when the one-loop effects are very large, higher order loops should also be considered. In Ref. [17] resummation techniques are proposed to improve the one-loop results.

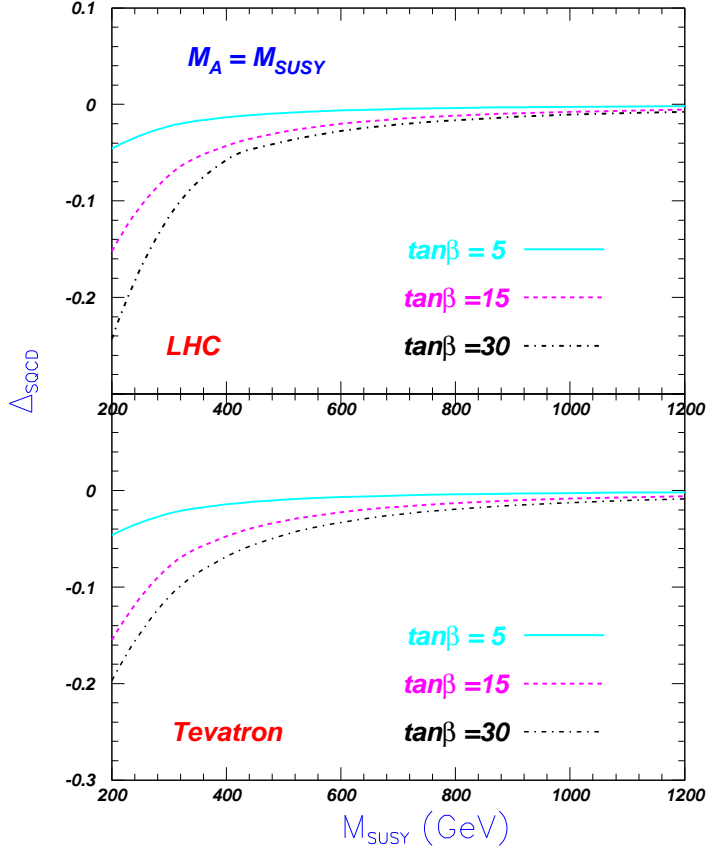


FIG. 5. Same as Fig.3 but with  $M_A = M_{SUSY}$ . The corresponding range of  $m_h$  is 94  $\sim$  116 GeV for  $\tan\beta = 5$ , 102  $\sim$  122 GeV for  $\tan\beta = 15$  and 103  $\sim$  123 GeV for  $\tan\beta = 30$ .

Note that in our calculations, instead of using the effective  $hb\bar{b}$  vertex [12], we performed the complete one-loop calculations for  $hb\bar{b}$  Yukawa coupling, which, as pointed out in the paragraph following eq.(4), are dependent on the external momenta of  $hb\bar{b}$  vertex. We found that when SUSY mass scale is larger than about 1 TeV, using the effective  $hb\bar{b}$  vertex [12] is a good approximation.

As we pointed out in the Introduction, we only considered the one-loop SUSY QCD corrections, which are the dominant part of the SUSY corrections. Of course, the SUSY electroweak corrections to  $hb\bar{b}$  coupling also have residue effects, which, however, are obviously suppressed by a factor  $\alpha_{EW}/\alpha_s$  relative to the SUSY QCD effects. Since much more parameters are involved in the SUSY electroweak sector, we did not perform a detailed calculation for the SUSY electroweak corrections here.

#### IV. CONCLUSION

We examined the supersymmetric QCD effects in bottom pair production associated with a light Higgs boson at the LHC and Tevatron. We found that when the relevant particles are heavy, well above the TeV scale, they nevertheless contribute sizable virtual effects in this process. For large  $\tan\beta$ , these residual effects can alter the production cross section by as much as 40 percent and thus should be measurable in observations of this process at the LHC or Tevatron.

If only one light Higgs boson, or perhaps several Higgs bosons, are discovered at the LHC or Tevatron, it could indicate that the SUSY scale is quite high; above the TeV scale. Of course, the fine-tuning problem then remains and supersymmetry loses one of its merits. But this might possibly happen since supersymmetry does not have to solve the fine-tuning problem, as argued recently by Arkani-Hamed and Dimopoulos [9]. In that case, a possible way to reveal a hint of supersymmetry is through its residue effects. Higgs production associated with a pair of bottom

quarks is then well suited for such a seeking a clue for supersymmetry.

## ACKNOWLEDGMENT

We thank Junjie Cao for discussions. This work is supported in part by the Chinese Natural Science Foundation and by the US Department of Energy, Division of High Energy Physics under grant No. DE-FG02-91-ER4086.

## APPENDIX A: EXPRESSIONS OF SUSY QCD CORRECTIONS TO THE AMPLITUDE

The coupling at the vertex  $h^0 \tilde{b}_i \tilde{b}_j^*$  is needed in our calculations. It is given by

$$V(h^0 \tilde{b}_i \tilde{b}_j^*) = igQ_{ij} , \quad (\text{A1})$$

where

$$Q_{11} = c_1 \cos^2 \theta_b + c_2 \sin^2 \theta_b + 2c_3 \sin \theta_b \cos \theta_b , \quad (\text{A2})$$

$$Q_{12} = (c_2 - c_1) \sin \theta_b \cos \theta_b + c_3 (\cos^2 \theta_b - \sin^2 \theta_b) , \quad (\text{A3})$$

$$Q_{21} = (c_2 - c_1) \sin \theta_b \cos \theta_b + c_3 (\cos^2 \theta_b - \sin^2 \theta_b) , \quad (\text{A4})$$

$$Q_{22} = c_1 \sin^2 \theta_b + c_2 \cos^2 \theta_b - 2c_3 \sin \theta_b \cos \theta_b , \quad (\text{A5})$$

with

$$c_1 = -\frac{m_Z}{\cos \theta_W} \left( \frac{1}{2} - \frac{1}{3} \sin^2 \theta_W \right) \sin(\alpha + \beta) , \quad (\text{A6})$$

$$c_2 = -\frac{m_Z}{\cos \theta_W} \frac{1}{3} \sin^2 \theta_W \sin(\alpha + \beta) , \quad (\text{A7})$$

$$c_3 = \frac{m_b}{2m_W \cos \beta} (A_b \sin \alpha + \mu \cos \alpha) . \quad (\text{A8})$$

Here  $\alpha$  is the mixing angle between the two neutral CP-even Higgs bosons. Then one-loop contributions  $\delta M^{q\bar{q}}$  and  $\delta M^{gg}$  are given by

$$\begin{aligned} \delta M_1^{q\bar{q}} = & \frac{-iG_S T_{ij}^a T_{kl}^a}{\hat{s}[(k_2 + k_3)^2 - m_b^2]} \bar{v}(p_1) \gamma^\mu u(p_2) \bar{u}(k_2) [(a_i - b_i \gamma^5)(-k_2 C_{11} - k_3 C_{12} + m_{\tilde{g}} C_0) \\ & \times (a_j + b_j \gamma^5) Q_{ij} - G\delta Z] (k_2 + k_3 + m_b) \gamma_\mu v(k_1) (-k_2, -k_3, m_{\tilde{g}}, m_{\tilde{b}_i}, m_{\tilde{b}_j}) , \end{aligned} \quad (\text{A9})$$

$$\begin{aligned} \delta M_2^{q\bar{q}} = & \frac{iG_S T_{ij}^a T_{kl}^a}{\hat{s}[(k_1 + k_3)^2 - m_b^2]} \bar{v}(p_1) \gamma^\mu u(p_2) \bar{u}(k_2) \gamma_\mu (k_1 + k_3 - m_b) [(a_i - b_i \gamma^5)(k_1 C_{11} \\ & + k_3 C_{12} + m_{\tilde{g}} C_0)(a_j + b_j \gamma^5) Q_{ij} - G\delta Z] v(k_1) (k_1, k_3, m_{\tilde{g}}, m_{\tilde{b}_i}, m_{\tilde{b}_j}) , \end{aligned} \quad (\text{A10})$$

$$\begin{aligned} \delta M_1^{gg} = & \frac{-G_S T_{ij}^c f_{abc}}{\hat{s}[(k_2 + k_3)^2 - m_b^2]} \bar{u}(k_2) [(a_i - b_i \gamma^5)(-k_2 C_{11} - k_3 C_{12} + m_{\tilde{g}} C_0)(a_j + b_j \gamma^5) Q_{ij} \\ & - G\delta Z] (k_2 + k_3 + m_b) \gamma^\lambda v(k_1) F_{\lambda\mu\nu} \varepsilon^\mu(p_1) \varepsilon^\nu(p_2) (-k_2, -k_3, m_{\tilde{g}}, m_{\tilde{b}_i}, m_{\tilde{b}_j}) , \end{aligned} \quad (\text{A11})$$

$$\begin{aligned} \delta M_2^{gg} = & \frac{G_S T_{ij}^c f_{abc}}{\hat{s}[(k_2 + k_3)^2 - m_b^2]} \bar{u}(k_2) \gamma^\lambda (k_1 + k_3 - m_b) [(a_i - b_i \gamma^5)(k_1 C_{11} + k_3 C_{12} + m_{\tilde{g}} C_0) \\ & \times (a_j + b_j \gamma^5) Q_{ij} - G\delta Z] v(k_1) F_{\lambda\mu\nu} \varepsilon^\mu(p_1) \varepsilon^\nu(p_2) (k_1, k_3, m_{\tilde{g}}, m_{\tilde{b}_i}, m_{\tilde{b}_j}) , \end{aligned} \quad (\text{A12})$$

$$\begin{aligned} \delta M_3^{gg} = & \frac{iG_S T_{ij}^b T_{jk}^a}{[(k_2 + p_2)^2 - m_b^2][(p_1 - k_1) - m_b^2]} \bar{u}(k_2) \gamma_\nu (k_2 - p_2 + m_b) [(a_i - b_i \gamma^5)(k_1 C_{11} \\ & - p_1 C_{11} + k_3 C_{12} + m_{\tilde{g}} C_0)(a_j + b_j \gamma^5) Q_{ij} - G\delta Z] \\ & \times (p_1 - k_1 + m_b) \gamma_\mu v(k_1) \varepsilon^\mu(p_1) \varepsilon^\nu(p_2) (k_1 - p_1, k_3, m_{\tilde{g}}, m_{\tilde{b}_i}, m_{\tilde{b}_j}) , \end{aligned} \quad (\text{A13})$$

$$\delta M_4^{gg} = \frac{iG_S T_{ij}^b T_{jk}^a}{[(k_2 + k_3)^2 - m_b^2][(p_1 - k_1) - m_b^2]} \bar{u}(k_2) [(a_i - b_i \gamma^5)(-k_2 C_{11} - k_3 C_{12}$$



$$+m_{\bar{g}}C_0)(a_j + b_j\gamma^5)Q_{ij} - G\delta Z](\not{k}_2 + \not{k}_3 + m_b)\gamma_\nu \\ \times (\not{p}_1 - \not{k}_1 + m_b)\gamma_\mu v(k_1)\varepsilon^\mu(p_1)\varepsilon^\nu(p_2)(-k_2, -k_3, m_{\bar{g}}, m_{\bar{b}_i}, m_{\bar{b}_j}) , \quad (\text{A14})$$

$$\delta M_5^{gg} = \frac{iG_S T_{ij}^a T_{jk}^b}{[(k_2 + p_1)^2 - m_b^2][(p_2 - k_1) - m_b^2]} \bar{u}(k_2)\gamma_\mu(\not{k}_2 - \not{p}_1 + m_b)[(a_i - b_i\gamma^5)(\not{k}_1 C_{11} \\ - \not{p}_2 C_{11} + \not{k}_3 C_{12} + m_{\bar{g}}C_0)(a_j + b_j\gamma^5)Q_{ij} - G\delta Z](\not{p}_2 - \not{k}_1 \\ + m_b)\gamma_\nu v(k_1)\varepsilon^\mu(p_1)\varepsilon^\nu(p_2)(k_1 - p_2, k_3, m_{\bar{g}}, m_{\bar{b}_j}, m_{\bar{b}_i}) , \quad (\text{A15})$$

$$\delta M_6^{gg} = \frac{iG_S T_{ij}^a T_{jk}^b}{[(k_2 + k_3)^2 - m_b^2][(p_2 - k_1) - m_b^2]} \bar{u}(k_2)[(a_i - b_i\gamma^5)(-\not{k}_2 C_{11} - \not{k}_3 C_{12} + m_{\bar{g}}C_0) \\ \times (a_j + b_j\gamma^5)Q_{ij} - G\delta Z](\not{k}_2 + \not{k}_3 + m_b)\gamma_\mu(\not{p}_2 - \not{k}_1 \\ + m_b)\gamma_\nu v(k_1)\varepsilon^\mu(p_1)\varepsilon^\nu(p_2)(-k_2, -k_3, m_{\bar{g}}, m_{\bar{b}_i}, m_{\bar{b}_j}) , \quad (\text{A16})$$

$$\delta M_7^{gg} = \frac{-iG_S T_{ij}^a T_{jk}^b}{[(k_2 - P_1)^2 - m_b^2][(k_1 + k_3) - m_b^2]} \bar{u}(k_2)\gamma_\mu(\not{k}_2 - \not{p}_1 + m_b)\gamma_\nu(\not{k}_1 + \not{k}_3 \\ - m_b)[(a_i - b_i\gamma^5)(\not{k}_1 C_{11} + \not{k}_3 C_{12} + m_{\bar{g}}C_0)(a_j + b_j\gamma^5)Q_{ij} \\ - G\delta Z]v(k_1)\varepsilon^\mu(p_1)\varepsilon^\nu(p_2)(k_1, k_3, m_{\bar{g}}, m_{\bar{b}_j}, m_{\bar{b}_i}) , \quad (\text{A17})$$

$$\delta M_8^{gg} = \frac{-iG_S T_{ij}^b T_{jk}^a}{[(k_2 - P_2)^2 - m_b^2][(k_1 + k_3) - m_b^2]} \bar{u}(k_2)\gamma_\nu(\not{k}_2 - \not{p}_2 + m_b)\gamma_\mu(\not{k}_1 + \not{k}_3 \\ - m_b)[(a_i - b_i\gamma^5)(\not{k}_1 C_{11} + \not{k}_3 C_{12} + m_{\bar{g}}C_0)(a_j + b_j\gamma^5)Q_{ij} \\ - G\delta Z]v(k_1)\varepsilon^\mu(p_1)\varepsilon^\nu(p_2)(k_1, k_3, m_{\bar{g}}, m_{\bar{b}_j}, m_{\bar{b}_i}) , \quad (\text{A18})$$

where we defined

$$a_{1,2} = (\sin\theta_b \mp \cos\theta_b)/\sqrt{2} , \quad (\text{A19})$$

$$b_{1,2} = (\cos\theta_b \pm \sin\theta_b)/\sqrt{2} , \quad (\text{A20})$$

$$F_{\lambda\mu\nu} = (p_1 - p_2)_\lambda g_{\mu\nu} + (p_2 + k_1 + k_2 + k_3)_\mu g_{\nu\lambda} - (p_1 + k_1 + k_2 + k_3)_\nu g_{\lambda\mu} . \quad (\text{A21})$$

In the above,  $p_1$  and  $p_2$  are respectively the momenta of the incoming quark and antiquark,  $k_1, k_2$  and  $k_3$  are respectively the outgoing  $b$  quark,  $\bar{b}$  quark, and the Higgs boson momenta,  $\hat{s}$  is the Mandelstam variable defined by  $\hat{s} = (k_1 + k_2 + k_3)^2 = (p_1 + p_2)^2$ ,  $T^a$  are the  $SU(3)$  color matrices,  $f_{abc}$  are anti-symmetric structure constants of  $SU(3)$  color matrices,  $G_S = gg_s^4 C_F/16\pi^2$  with  $C_F = 4/3$ , and  $C_0$  and  $C_{ij}$  are the 3-point Feynman integrals [15] with their functional dependence indicated in the brackets following them.

- [1] For a review, see, e.g., H. E. Haber, G. L. Kane, Phys. Rept. **117**, 75 (1985).
- [2] D. Dicus, T. Stelzer, Z. Sullivan, S. Willenbrock, Phys. Rev. D **59**, 094016 (1999).
- [3] C. Balazs, H.-J. He, C. P. Yuan, Phys. Rev. D **60**, 114001 (1999).
- [4] J. Campbell, R. K. Ellis, F. Maltoni, S. Willenbrock, Phys. Rev. D **67**, 095002 (2003).
- [5] S. Dittmaier, M. Krämer, M. Spira, Phys. Rev. D **70**, 074010 (2004).
- [6] S. Dawson, C. Jackson, L. Reina, D. Wackerroth, Phys. Rev. D **69**, 074027 (2004).
- [7] S. Dawson, C. B. Jackson, L. H. Orr, L. Reina, D. Wackerroth, hep-ph/0311105.
- [8] D. Dicus, S. Willenbrock, Phys. Rev. D **39**, 751 (1989).
- [9] N. Arkani-Hamed and S. Dimopoulos, hep-th/0405159.
- [10] L. Senatore, hep-ph/0412103.
- [11] H. E. Haber, et al., Phys. Rev. D **63**, 055004 (2001).
- [12] A. Dabelstein, Nucl. Phys. **B456**, 25 (1995); C. S. Li, J. M. Yang, Phys. Lett. B **315**, 367(1993); For a review, see, M. Carena and H. E. Haber, Prog.Part.Nucl.Phys. **50** 63 (2003).
- [13] J. Cao, G. Gao, R. J. Oakes, J. M. Yang, Phys. Rev. D **68**, 075012 (2003).
- [14] G. Gao, G. Lu, Z. Xiong and J. M. Yang, Phys. Rev. D **66**, 015007 (2002).
- [15] G. Passarino and M. Veltman, Nucl. Phys. **B160**, 151 (1979).

- [16] See, for example, E. Braaten and J. P. Leveille, Phys. Rev. **D22**, 715 (1980); M. Drees and K. Hikasa, Phys. Lett. B**240**, 455 (1990).
- [17] M. Carena, D. Garcia, U. Nierste and C. E. Wagner, Nucl. Phys. **B577**, 88 (2000); H. Eberl, *et al.*, Phys. Rev. D **62**, 055006 (2000).
- [18] H. L. Lai, *et al.* (CTEQ collaboration), Eur. Phys. J. C**12**, 375 (2000).
- [19] J. F. Gunion and H. E. Harber, Nucl. Phys. **B272**, 1 (1986).
- [20] H. N Brown, *et al.*, Mu g-2 Collaboration, Phys. Rev. Lett. **86**, 2227 (2001).
- [21] Particle Physics Group. Eur. Phys. J. C**15**, 274 (2000).
- [22] For some early discussions, see, e.g, X. Y. Li, E. Ma, J. Phys. G **23**, 885 (1997).
- [23] A. Dobado, M. J. Herrero, D. Temes, Phys. Rev. D **65**, 075023 (2002).
- [24] W. Beenakker, *et al.*, Phys. Rev. Lett. **87**, 201805 (2001).
- [25] L. Reina and S. Dawson, Phys. Rev. Lett. **87**, 201804 (2001).
- [26] W. Beenakker, *et al.*, Nucl. Phys. **B653**, 151 (2003).
- [27] L. Reina, S. Dawson and D. Wackeroth, Phys. Rev. D **65**, 053017 (2002).
- [28] S. Dawson, L. H. Orr, L. Reina and D. Wackeroth, Phys. Rev. D **67**, 071503 (2003).
- [29] S. Dawson, C. Jackson, L. H. Orr, L. Reina and D. Wackeroth, Phys. Rev. D **68**, 034022 (2003).